Supporting Information

Defective Silicotungstic acid-loaded magnetic floral N-doped carbon microspheres for ultra-fast oxidative desulfurization of high sulfur liquid fuels

Yefeng Liu [a,b]*, Xiaojie Yin [a], Chuan Li [a], Zhong Xie [a], Fuyan Zhao [a], Jing Li[a], Jinpei Hei [a], Yang Han [a], nannan Wang[a]*, Peng Zuo[a],*

a. Engineering Technology Research Center of Preparation and Application of Industrial Ceramics of Anhui Province, School of Chemistry and Material Engineering, Chaohu University, 1 Bantang Road, Chaohu, P. R. China, 238000

b. Engineering Research Center of High-frequency Soft Magnetic Materials and Ceramic Powder Materials of Anhui Province, Chaohu University, Chaohu 238000, P. R. China, 238000.

Corresponding author e-mail: lyf@chu.edu.cn (Yefeng Liu); nnw1990@126.com (nannan Wang); zp@chu.edu.cn (Peng Zuo)

1. Materials

Silicotungstic acid ($H_4SiW_{12}O_{40} \cdot xH_2O$, abbreviated as SiW_{12}), $H_3PW_{12}O_{40} \cdot xH_2O$ (abbreviation for PW_{12}) and Phosphomolybdic acid ($H_3PMo_{12}O_{40} \cdot xH_2O$, abbreviated as PMo_{12}) were purchased from Shanghai Macklin Biochemical Co., Ltd. (Jiangsu, China); Fe_3O_4 nanoparticle particles (20 nm) and

dopamine hydrochloride (DA) were obtained from Shanghai Macklin Biochemical Co., Ltd. (Jiangsu, China); tris (hydroxymethyl) aminomethane ($C_4H_{11}NO_3$, Tris) was obtained from Shanghai Aladdin Bio-Chem Technology Co., Ltd. (Jiangsu, China); Dibenzothiophene (DBT), benzothiophene (BT), and 4,6-dimethyldibenzothiophene (4,6-DMDBT) were purchased from Aladdin Bio-Chem Technology Co., Ltd. (Jiangsu, China); N-octane and acetonitrile were obtained from Tianjin Damao Chemical Reagent Factory (Tianjin, China); other drugs and reagents are commercially available analytically pure.

2. Characterization

Fourier transform infrared (FT-IR) spectra were carried out on a L1600300 Spectrum Two LITa infrared spectrometer (UK) using the KBr pellet approach. Ultraviolet-Visible spectra of the samples were obtained on a 2802 UV/Vis instrument (Youniko, Shanghai). X-ray photoelectron spectroscopy (XPS) was measured on a Thermo Fisher Scientific Escalab 250Xi X-ray photoelectron Spectrometer (American) using Al Ka radiation and the C1s peak at 284.8 eV as internal standard. The X-ray diffraction (XRD) measurements of all samples were collected with Bruker D8 Advance X-ray powder diffractometer (Germany) using a Cu Kα source to determine the chemical composition and crystalline structural properties of the samples. Scanning electronic microscopy (SEM) was determined with a Hitachi S4800 / FEI NANOSEM 450 microscope (USA). Energy-dispersive X-ray spectroscopy (EDX) analytical data were acquired on EDAX Apollo XT spectrometer (USA). Thermogravimetry analyser (TG) was conducted by a NETZSCH STA 449 F3 analyzer (Germany) in air condition from room temperature to 900 °C, with a change of 10 °C min^{-1}. The activate radicals were recorded from by EPR (MiniSpcope MS 5000, Magnettech, Germany) with 5,5-dimethyl-1-pyrrolidine-N-oxide (DMPO) as electron capturing reagent. Tungsten content was tested by inductively-coupled plasma optical

emission spectrometry (ICP-OES, Agilent 5110, USA). The H_2 temperature-programmed reduction (H_2-TPR, MFTP3060, China) was performed with a heating rate of 10 °C/min in a 5 % H_2/Ar flow (50 cm^3/min). Prior to monitoring of the TPR profiles, 100 mg of the samples were placed in a quartz reactor and heated at 200 °C in an argon flow for 60 min. High performance liquid chromatograph (HPLC, LC98-I, Beijing Wenfen Analysis Instrument Technology Development Co., Ltd) was used to confirm the ODS reaction product.

3. The test condition of HPLC for ODS reaction

C18 reversed-phase column (200 mm×4.6 mm×5 µm ID), column temperature of 30 °C, test wavelength of 254 nm. The mobile phase was methanol/H_2O (90/10, V/V) with flow rate of 1.0 mL·min^{-1}.

4. Kinetic studies of ODS, the apparent activation energy and TOF

The value of kinetic constant (k) given in Fig. 7 b can be obtained by the following equation:

$$\ln\frac{C_0}{C_t} = kt \tag{1}$$

where k represents the rate constant, t is the reaction time, C_0 is the initial sulfur content of the model oil, and C_t is the sulfur content at time t.

The plot of ln k against 1/T is shown in Fig. 7 c according to the Arrhenius equation (2).

$$\ln k = -\frac{E_a}{RT} + \ln A \tag{2}$$

Based on the linear correlation between -ln k and 1/T displayed in Fig. 7 c, the obtained linear equation is y=4665.36x-12.550, the estimated value of Ea is 38.79 kJ/mol.

where E_a is the apparent activation energy, kJ / mol; R is the molar gas constant, J / (mol·K); T is the thermodynamic temperature, K; A is the pre-exponential factor; and k is the reaction rate constant, min^{-1}.

$$TOF = \frac{mole\ number\ of\ converted\ DBT}{mole\ of\ active\ species\ content\ in\ catalyst \times reaction\ time(h)} \quad (3)$$

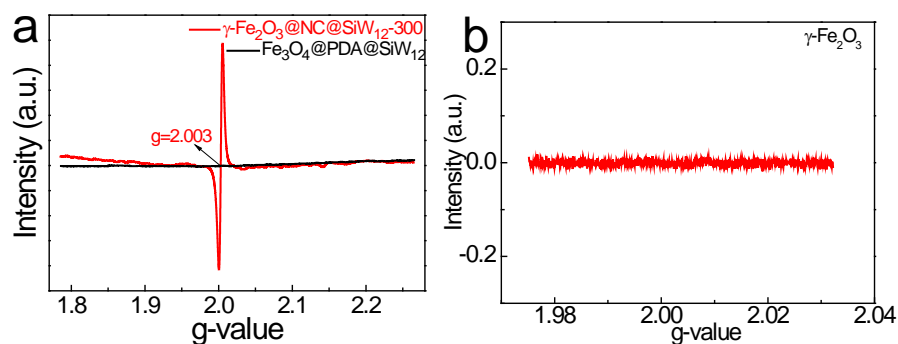Fig. S1 EPR spectra of (a) γ-Fe$_2$O$_3$@NC@SiW$_{12}$-300 and Fe$_3$O$_4$@PDA@SiW$_{12}$ and (b) γ-Fe$_2$O$_3$
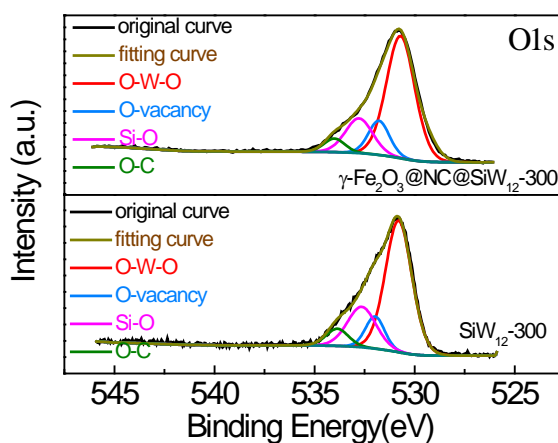
Fig. S2 XPS spectra of O1s of γ-Fe$_2$O$_3$@NC@SiW$_{12}$-300 and SiW$_{12}$-300
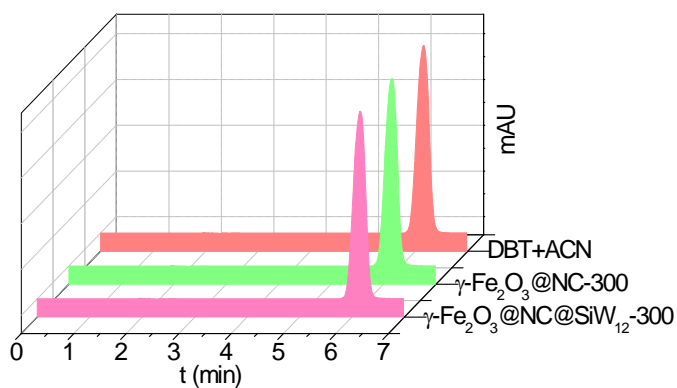
Fig. S3 Model oils containing DBT+ACN system added with γ-Fe$_2$O$_3$@NC-300 and γ-Fe$_2$O$_3$@NC@SiW$_{12}$-300,

respectively.
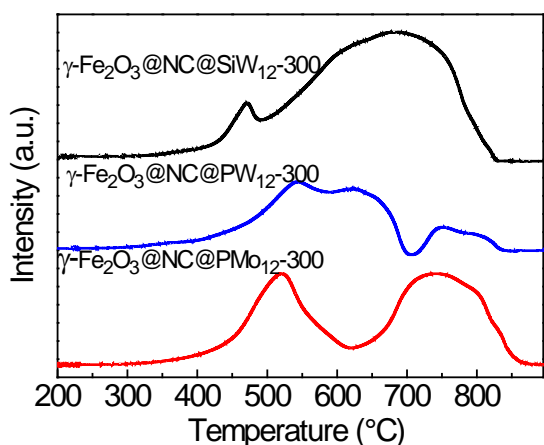
Fig. S4 H_2-TPR spectra of γ-Fe_2O_3@NC@SiW$_{12}$-300, γ-Fe_2O_3@NC@PW$_{12}$-300 and γ-Fe_2O_3@NC@PMo$_{12}$-300.
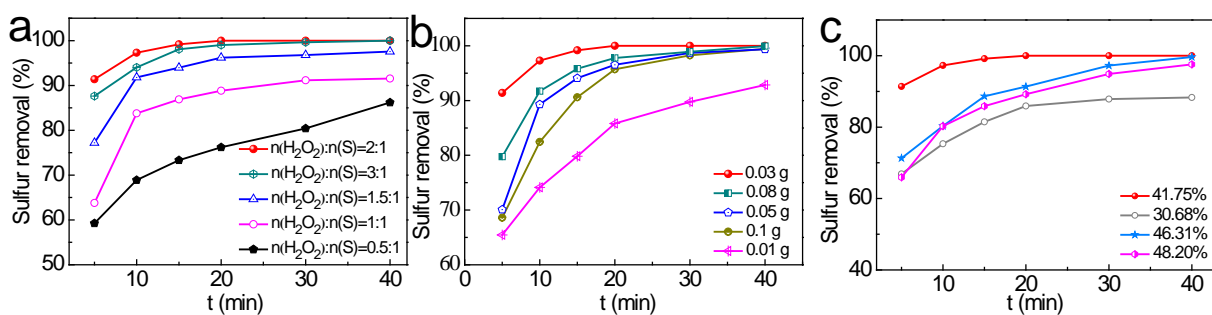

Fig. S5 (a) Effects of H_2O_2 dosage on the sulfur removal rate (0.03 g catalysts; T = 60 ℃); (b) Effects of catalyst dosage on the sulfur removal rate (n(H_2O_2) : n(S) = 2:1; T = 60 ℃); (C) Effects of the loading amount of SiW$_{12}$ on the sulfur removal rate (0.03 g catalysts; n(H_2O_2) : n(S) = 2:1; T = 60 ℃)
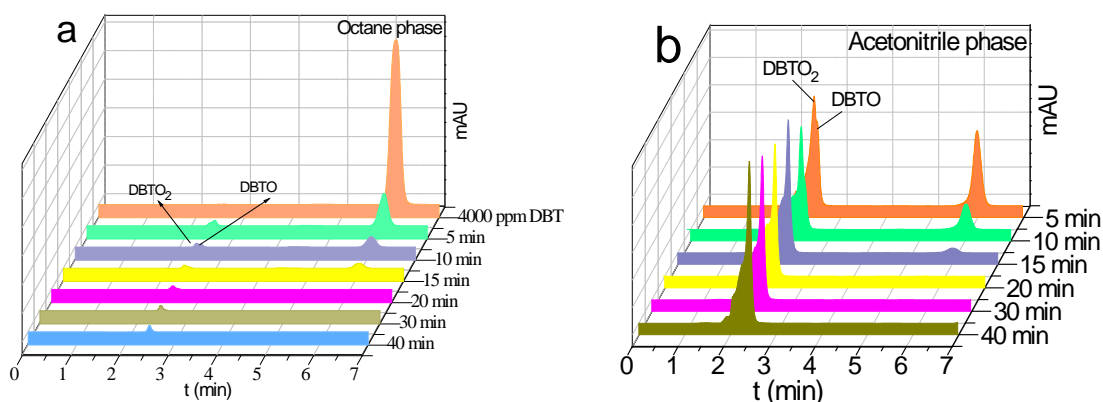

Fig. S6 HPLC chromatograms of (a) n-octane phases (b) and acetonitrile phases for ODS over γ-Fe_2O_3@NC@SiW$_{12}$-300 with H_2O_2 as oxidant.
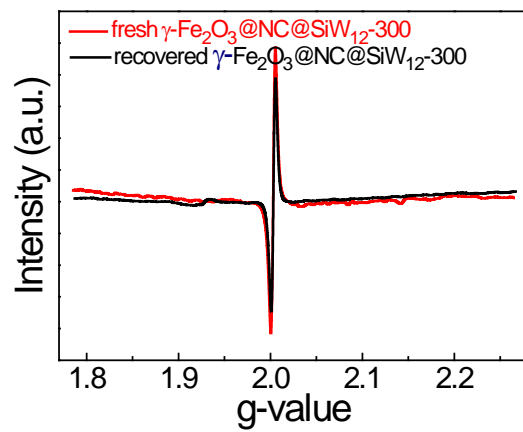
Fig. S7 EPR spectra of fresh and recovered γ-Fe$_2$O$_3$@NC@SiW$_{12}$-300 catalyst